

CAPACITY OPTIMIZATION OF ADVANCED ENERGY STORAGE TECHNOLOGIES FOR PEAK SHAVING AND FREQUENCY REGULATION BASED ON ECONOMIC AND CARBON-MITIGATION CO-BENEFIT

Lu Nie¹, Yanxin Li¹, You Gan¹, Xiaoqu Han^{1*}, Tong Wang², Junjie Yan¹

¹State Key Laboratory of Multiphase Flow in Power Engineering, Xi'an Jiaotong University, Xi'an, China

²Huadian Electric Power Research Institute Co., Ltd., Beijing, China

*Xiaoqu Han: hanxiaoqu@mail.xjtu.edu.cn

ABSTRACT

With the rapid scale-up in popularity of renewable energy sources, the new power system is suffering from enhanced instability. In order to improve flexibility of new power system and mitigate carbon emission, the integration of thermal power plants with energy storage technologies (ESTs) has gradually become a promising solution. As a key support for the development of new power system, it is of great significance to investigate the capacity optimization of advanced ESTs. However, there was a lack of study related to the capacity optimization of ESTs and the combination revenue patterns of ESTs were seldom considered. In the present work, a capacity optimization model was established for ESTs operating in combination with thermal power plants on the generating side, including lithium iron phosphate battery (LIPB), vanadium redox flow battery (VRFB), compressed air energy storage (CAES), supercapacitors (SC), and flywheel (FE) with the goal of maximizing the co-benefit. LIPB, VRFB, and CAES energy storage systems were investigated in the peak shaving (PS) scenario. The co-benefit of ESTs was significant, 30.7-43.2 \$/MWh, internal rate of return (IRR) was 12%-20%, and payback period (PP) was 6-11 years when the ratio of ESTs allocation (EAR) for thermal power plants was 2.50%-5.52%. LIPB, VRFB, CAES, SC, and FE were investigated in the frequency regulation (FR) scenario. The co-benefit of ESTs was 51.9-329.3 \$/MWh, IRR was 20%-35%, and PP was 3-7 years when the EAR was 0.24%-5.65%. The contribution of carbon mitigation benefit to co-benefit for different ESTs varied substantially, ranging from 6.46% to 82.75%. The ESTs not only offered ancillary service, but also other services when it operated as an independent shared energy storage. A new combination revenue pattern was proposed, under which revenue increased by 35%-55% compared to that of existing patterns. Sensitivity analysis was performed, in which the cost of energy storage, carbon tax, peak-valley spread, and comprehensive regulation performance indexes had a significant impact on co-benefit. The results could provide optimization strategies and recommendations for energy storage capacity allocation and co-benefit enhancement of new power system.

1 INTRODUCTION

In order to mitigate carbon emission and ensure energy security, countries around the world have embarked on strategies to transform their energy mix. New power system is significantly increasing the installed capacity of renewable energy (Arbabzadeh et al., 2019, Jiao et al., 2023). Power system requires additional flexibility to ensure that renewable energy can be efficiently integrated into new power system, as renewable energy is an intermittent and volatile resource (Dreidy et al., 2017). Therefore, new regulation measures to assist traditional plants to balance the power volatility have become the focus of research. Wang et al. (2022) outlined the application scenarios of various energy storage technologies (ESTs) and analyzed their ability to solve the problem of renewable energy fluctuations. Thermal power plants are the backbone of power system supply stability in China, but the dispatch instructions for thermal units are slow and there is a zone of speed regulation insensitivity.

Advanced EST with fast response speed, high regulation accuracy and flexible layout is an important support for the construction of new power system (Koochi-Fayegh et al., 2020, Fang et al., 2022).

Studies on the economic assessment of ESTs in multiple scenarios were available (Bradbury et al., 2014, Zakeri et al., 2015). Mostafa et al. (2020) presented a cost model of ESTs from the perspective of long, medium, and short-term applications. A review of cost and benefit modeling of energy storage systems was presented by Hittinger et al. (2020). In addition, He et al. (2016) investigated the optimal tendering policy for ESTs in the electricity market with the goal of maximizing benefit. Rayit et al. (2021) examined ESTs for the provision of grid-scale energy services, from both a technical and economic perspective. Wu et al. (2022) investigated the capacity and operation optimization of grid-side battery ESTs for FR and energy arbitrage. However, the comprehensive value of ESTs is not limited to economic benefit, but also carbon mitigation benefit. There were numerous studies available regarding the environmental effects of ESTs in different application scenarios (Ryan et al., 2018, Rahman et al., 2021). Miller et al. (2018) and Jiao et al. (2023) assessed the life cycle GHG emission of renewable power systems. Replacement of conventional units with energy storage technology is beneficial in reducing carbon emission. Replacing gas turbines with batteries reduced GHG emission by 87% (Chowdhury et al., 2020). However, a few studies monetized the benefit of carbon mitigation. Arbabzadeh et al. (2019) investigated the ability of energy storage to reduce the amount of abandoned renewable energy and carbon emissions under different carbon tax policies. Dong et al. (2019) evaluated the economic values of GHG emission for three LCA methods. In a portion of studies on capacity optimization of ESTs, the cost of carbon emission was considered (Elzein et al., 2019, Tian et al., 2021). Schram et al. (2020) conducted Pareto optimization of cost and carbon emission targets for community energy storage systems. Li et al. (2023) investigated the comprehensive application of EST in peak shaving (PS) and FR, and the environmental benefit was considered in their techno-economic assessment model. Therefore, there was a lack of studies that combined the capacity optimization of ESTs with co-benefit.

Moreover, ESTs can offer not only ancillary services, but also other multi-application services as independent shared energy storage. They can participate in the electricity spot market or be leased while participating in the ancillary services market. ESTs that offer different services in a shared energy storage model can enhance profitability (Lombardi et al., 2017). However, the combination revenue patterns of the ESTs were rarely considered. The issues of optimal energy dispatch and reasonable profit distribution of shared energy storage have been sorted out (Kong et al., 2023). Shi et al. (2018) performed joint optimization of batteries operating in PS and FR. Zhang et al. (2020) investigated planning the entire life cycle of ESTs to provide multiple services. The results of the studies all indicated that batteries provided a wide range of services with significant economic benefit.

In the present work, a capacity optimization model was established for advanced ESTs operating in combination with thermal power plants on the generating side. The co-benefit of advanced ESTs, including lithium iron phosphate battery (LIPB), vanadium redox flow battery (VRFB), compressed air energy storage (CAES), supercapacitors (SC), and flywheel (FE) researched as objects in the work, in the PS and FR were studied. A combination revenue pattern for shared energy storage was proposed and different revenue patterns were analyzed. Furthermore, sensitivity analysis was performed to examine the impact of the critical parameters. The results could provide optimization strategies and recommendations for capacity allocation and co-benefit enhancement of ESTs in new power system.

2 METHODOLOGY

2.1 Applications and Cases

In theory, ESTs are available to meet many kinds of needs. The installed capacity on the power generation side accounts for the highest proportion of the one added in EST projects both in the world and China. Currently, EST is applied widely in joint operation with thermal power plants. Therefore, typical thermal power plant and EST joint operation projects in China were used as cases to investigate the scenarios in which EST assisted thermal power plants PS and FR. In addition, a combination of

revenue pattern for independent shared energy storage is investigated. The various benefit patterns of ESTs including ancillary services, participation in the electricity spot market, capacity leasing, and capacity compensation were displayed in Figure 1.

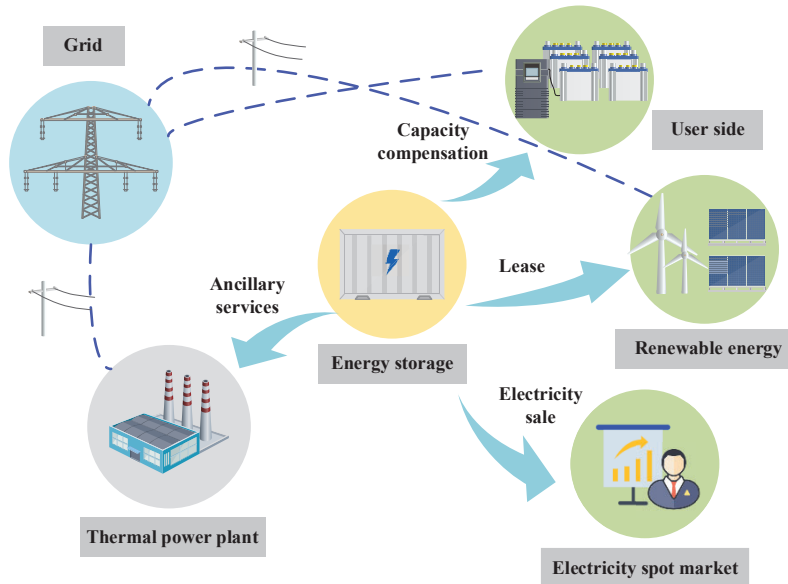


Figure 1: Overview of various benefit patterns of ESTs

2.2 Capacity Optimization Model

A capacity optimization model for ESTs assisting thermal power plants in PS or FR has been developed using generation and demand data from typical thermal power plants in China, details of which were shown in Figure 2.

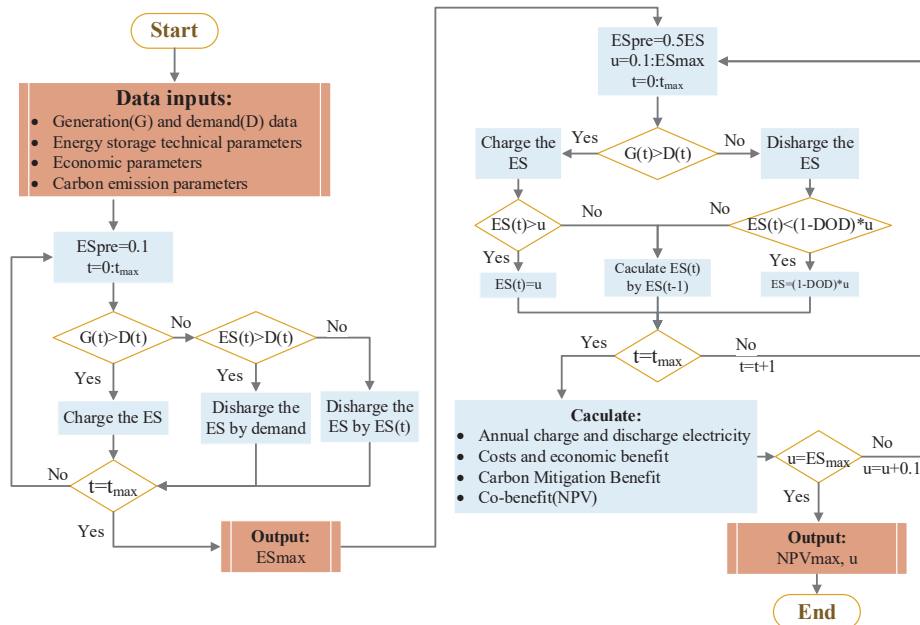


Figure 2: Capacity optimization flowchart

The gap between the thermal power plant's generation and the demand is the mismatched power, represented by the Equation (1).

$$\Delta W(t) = G(t) - D(t) \tag{1}$$

where $\Delta W(t)$ is the mismatched power at time t , $G(t)$ is the electricity generation at time t , and $D(t)$ is the demand for electricity at time t .

The charge and discharge of ESTs can be calculated as Equation (2).

$$\begin{cases} ES(t) = ES(t-1) \times (1 - \eta_{self}) + \eta_{ac} \times \Delta W(t) & \Delta W \geq 0 \\ ES(t) = ES(t-1) \times (1 - \eta_{self}) + \Delta W(t) / \eta_{ad} & \Delta W < 0 \end{cases} \tag{2}$$

where $ES(t)$ is the electricity quantity at time t , $ES(t-1)$ is the electricity quantity at time $t-1$, η_{self} is self-discharge rate, η_{ac} is charge efficiency, and η_{ad} is discharge efficiency.

After the execution of the model presented in Equation (2) over a certain duration, the computation of the infinitely large storage capacity becomes feasible by utilizing Equation (3), when the highest and lowest levels of content in the storage of unlimited size are considered. Equation (3) proves to be valid when the average reserve demand is larger than the average reserve energy stored. However, Equation (4) can be used to size storage when the average surplus generation exceeds the average surplus demand (Chowdhury et al., 2020).

$$ES_{max,inf} = \max[ES(t)] - \min[ES(t)] \tag{3}$$

$$ES_{max,fin} = \max_t [ES(t) - \min_{t'>t} ES(t')] \tag{4}$$

where $ES(t')$ is the electricity quantity at time t' ($t'>t$). The gap between $ES(t)$ and $\min ES(t')$ is the instantaneous storage energy at time t .

However, in practice the DOD of the EST will not reach 100%. Assuming that the real size is 110% of the size calculated by the equation, the maximum capacity of the EST is defined as follows:

$$ES_{max} \begin{cases} = 1.1 \times [1 + (1 - DOD) / \eta_{ad}] \times ES_{max,fin} & ES_{max,fin} \neq 0 \\ = 1.1 \times [1 + (1 - DOD) / \eta_{ad}] \times ES_{max,inf} & ES_{max,fin} = 0 \end{cases} \tag{5}$$

where DOD is the depth of discharge.

The co-benefit of configuring EST by the ES_{max} may not be maximum. To find the capacity size with maximum co-benefit, for each capacity from zero to ES_{max} , the charging, discharging, cost, and benefit were calculated. The electricity level and charge/discharge are restricted by Equations (6) and (7), respectively.

$$\begin{cases} ES(t) = \min[ES(t-1) \times (1 - \eta_{self}) + \eta_{ac} \times \Delta W(t), u] & \Delta W \geq 0 \\ ES(t) = \max[ES(t-1) \times (1 - \eta_{self}) + \eta_{ad} \times \Delta W(t), u \times (1 - DOD)] & \Delta W < 0 \end{cases} \tag{6}$$

$$\begin{cases} CE(t) = \min[(u - ES(t-1) + ES(t-1) \times \eta_{self}) / \eta_{ac}, \Delta W(t)] & \Delta W \geq 0 \\ DE(t) = \min\{[ES(t-1) - u \times (1 - DOD)] \times \eta_{ad}, -\Delta W(t)\} & \Delta W < 0 \end{cases} \tag{7}$$

where $CE(t)$ is the charging electricity at time t , $DE(t)$ is the discharging electricity at time t , u is the capacity of the EST.

The results of the simulated operation were then amplified over the entire lifespan of the EST for the co-benefit calculation. Costs, economic benefit, and carbon mitigation benefit were calculated for each EST over its entire life cycle by discounting them to present value.

The cost of EST included initial investment cost (C_{in}), operation and maintenance cost, replacement cost and recovery of salvage value. The initial investment cost is calculated by Equation (8) and the total cost is expressed by Equation (9).

$$C_{in} = P_c \times u / dura + E_c \times u \tag{8}$$

$$C = C_{in} + \sum_{i=1 \dots N} \mu \times C_{in} / (1+r)^i + C_R \times u \times (1-\tau)^j / (1+r)^j - \gamma \times C_{in} / (1+r)^N \quad (9)$$

Where P_C is power cost, E_C is energy cost, $dura$ is discharge duration, r is discount rate, i represents the year, j represents the year to be replaced, τ is the cost reduction rate, 7.78%, C_R is unit replacement cost, γ is salvage value, and N is life of the power station.

ESTs obtained benefit in different ways when offering in different ancillary services. Benefit was obtained through peak-valley arbitrage and policy subsidies in PS, as written in Equation (10). In FR, ESTs obtained benefit from mileage and capacity compensation, which were given by Equation (11).

$$R_{PS} = \sum_{i=1 \dots N} D_{ES} \times P(t) / (1+r)^i + B_{PS} \times B_{PST} \times D_{ES} \quad (10)$$

$$R_{FR} = \sum_{i=1 \dots N} (B_{mil} \times K \times S_{mil} + S_{fc} \times B_{cap}) / (1+r)^i \quad (11)$$

where D_{ES} represents annual discharge, $P(t)$ is price of electricity at different times, B_{PS} is peaking subsidy, B_{PST} is duration of the subsidy, B_{mil} is FR mileage subsidy, K is comprehensive regulation performance indicator, S_{mil} is annual FR mileage, S_{fc} is annual FR capacity, and B_{cap} is FR capacity subsidy.

ESTs assisted thermal power plants in PS or FR, and the produced electricity in this way could replace the part that should be generated by thermal power plants, indirectly realizing the value of carbon mitigation. The carbon mitigation benefit can be determined from the Equation (12).

$$S = \sum_{i=1 \dots N} D_{ES} \times \lambda_{CO_2} \times T_c / (1+r)^i \quad (12)$$

where λ_{CO_2} is CO₂ emission factor, and T_c is carbon tax.

Co-benefit was given by Equation (13).

$$NPV = (R_{PS} \text{ or } R_{FR}) + S - C \quad (13)$$

The iterative process was performed separately for each capacity to determine the maximum co-benefit as well as the corresponding capacity. In addition, calculating the corresponding internal rate of return (IRR) and payback period (PP) to determine if the project was well-benefited.

IRR is the new discount rate, which is the value of the discount rate that results in zero NPV over the life of the project. PP is the period that makes the difference between cost and benefit equal to zero as shown in Equation (14).

$$\sum_{i=0}^{PP} (R_{PS} \text{ or } R_{FR}) + S = \sum_{i=0}^{PP} C \quad (14)$$

2.3 Benefit Patterns for Shared Energy Storage

The ESTs not only offered ancillary service, but also other services when it operated as an independent shared energy storage. Taking the independent shared energy storage plant in China as an example, it can be leased to new energy enterprises to obtain benefit (R_L), purchase and sell electricity in the electricity spot market to obtain electricity differentials (R_M), and obtain a certain amount of capacity compensation (R_C). These three types of benefit were respectively represented as Equation (15,16,17).

$$R_L = \sum_{i=1 \dots N} u / dura \times k_l / (1+r)^i \quad (15)$$

$$R_M = \sum_{i=1 \dots N} \eta_{ac} \times \eta_{ad} \times u / dura \times k_m / (1+r)^i \quad (16)$$

$$R_C = \sum_{i=1 \dots N} u / dura \times k_c / (1+r)^i \quad (17)$$

where k_l is the annual capacity lease price, k_m is the average spot spread price, and k_c is the capacity compensation price.

Shared energy storage benefit patterns that have been realized in China were presented in Table 1, from the perspective of offering different ancillary services. In China, shared energy storage power plants still have the right to operate independently even if they are leased to renewable energy enterprises. Therefore, a fourth integrated model was proposed with an optimistic perspective to obtain four types of benefit.

Table 1: Independent shared energy storage benefit patterns

Types of ancillary services	benefit pattern	promotion region
PS	P1: R_{PS}	nationwide
	P2: R_{PS}, R_L	Hunan Province, Ningxia Province
	P3: R_L, R_M, R_C	Shandong Province
FR	P1: R_{FR}	Shanxi Province
	P2: R_{FR}, R_M	Shanxi Province
	P3: R_L, R_M, R_C	Shandong Province

3 RESULTS AND DISCUSSIONS

3.1 Capacity Optimization and Allocation

ESTs were investigated to offer PS and FR ancillary services for 600 MW and 300 MW thermal power plants, respectively. The technical and economic parameters of ESTs in each scenario were indicated in Table 2. Some technical data were based on our previous work (Han et al., 2023). Economic data obtained from Chinese manufacturers of ESTs. The capacity of the EST was obtained from the capacity optimization model, and the power was configured on the basis of the discharge duration, which provided a complete result of allocation ESTs. In this way, the ratio of ESTs allocation (EAR) of thermal power plants can be calculated and was given in Figure 3. This ratio is generalizable to the study of offering the same auxiliary services for thermal power plants.

Table 2: Technical and economic parameters of ESTs

Parameter	Units	PS			FR			SC	FE
		LIPB	VRFB	CAES	LIPB	VRFB	CAES		
Charge/discharge efficiency (η_{ac}/η_{dc})	%	92	80	60	92	80	60	90	90
Depth of discharge (DOD)	%	90	90	60	5	5	5	5	5
Life of the power station (N)	year	25	20	40	24	20	40	15	20
Calendar life of ESTs (N_E)	year	15	20	40	4	20	40	15	20
Discharge duration ($dura$)	h	2	4	4	0.5	2	2	0.17	0.25
Self-discharge rate (η_{self})	month	0.03	0.04	/	0.03	0.04	/	0.54	0.10
Power cost (P_c)	\$/kW	56	31	136	56	31	136	168	259
Energy cost (E_c)	\$/kWh	182	420	280	182	420	280	1522	700
operational and maintenance cost (μ)	%	1.5	2.5	1.5	1.5	2.5	1.5	1.5	1.5
Replacement cost (C_R)	\$/kWh	92	/	/	92	/	/	/	/

The most optimal capacities of ESTs obtained from the capacity optimization model were 66.2 MWh, 60.1 MWh, and 78.9 MWh for LIPB, VRFB, and CAES in PS scenario respectively. The discharge duration is different for different ESTs and scenarios. VRFB and CAES are long time storage technologies, whose discharge durations can even be up to 8 h in some advanced projects. According to the current data of most commercialized projects, the discharge duration of LIPB was 2 h, and the discharge duration of VRFB and CAES was 4 h, which resulted in the power allocation of 33.1 MW, 15.0 MW, and 19.7 MW, respectively. Therefore, the EARs for the three ESTs were 5.52%, 2.50%, and 3.29%. Short-duration, high-frequency power-based ESTs were suitable for FR scenario. The optimal capacities of LIPB, VRFB, CAES, SC, and FE in FR scenario were 3.90 MWh, 1.24 MWh, 1.44 MWh, 2.88 MWh, 2.89 MWh, respectively. The powers of SC and FE were 17 MW and 12 MW, which were significantly higher compared with other ESTs, and the EARs of VRFB and CAES were 0.21% and 0.24%, which were at a low level. Comparing the two scenarios, the EARs of LIPB, VRFB, and CAES were higher in PS scenario than in the FR scenario, which demonstrated that there was a high demand in the PS scenario for the capacity of the ESTs.

There is a lack of studies on the ratio of energy storage capacity configured for thermal plants, and most of the commercialized projects were based on the value of engineering experience, 3%-6%, to allocate EST for thermal plants. The results showed that most of the EARs were between 2.60%-5.65%, except for the FR scenario where the EARs for VRFB and CAES were less than 1%, since the advantage of VRFB and CAES was the long discharge duration, which was unprofitable if they were allocated too large power.

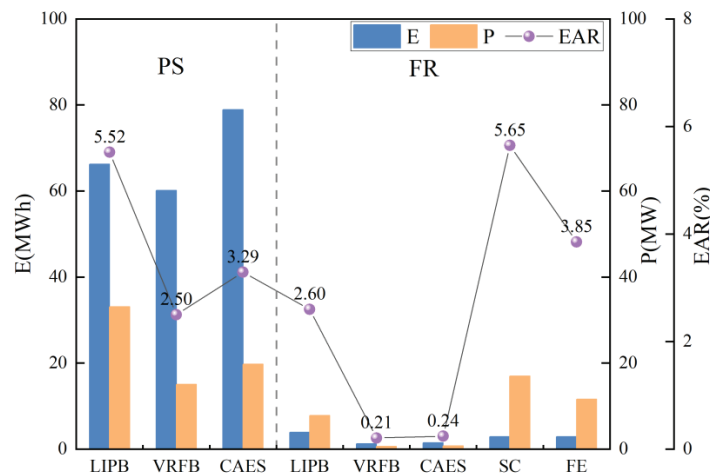


Figure 3: Capacity optimization and ESTs allocation results

3.2 Economic Performance

The costs and benefit of each EST in each scenario were calculated by unit-capacity EST, as plotted in Figure 4. In the comparison of the two scenarios, the NPV of LIPB, VRFB, and CAES were more in FR than in PS. The costs of SC and FE were significantly higher than other ESTs. In PS, the NPV of unit-capacity EST from the largest to the smallest were LIPB, CAES, and VRFB. The NPV of LIPB was at 37 \$/MWh. The economic benefit of the VRFB was highest, but its high cost rendered the NPV the lowest. In FR, the NPV of unit-capacity EST from the largest to the smallest were SC, FE, LIPB, CAES, and VRFB. The NPV of SC and FE were higher compared with other ESTs, and the one of FE, 340 \$/MWh, was the largest. In PS, carbon mitigation benefit accounted for 14%-26% of all benefit. In FR, carbon mitigation benefit of LIPB, VRFB, and CAES accounted for 15%-60% and SC and FE accounted for only 5%-7%. This was mainly due to the unit capacity EST of SC and FE characterized by high power and FR mileage for realizing economic benefit. The great economic benefit made the carbon mitigation benefit a small percentage.

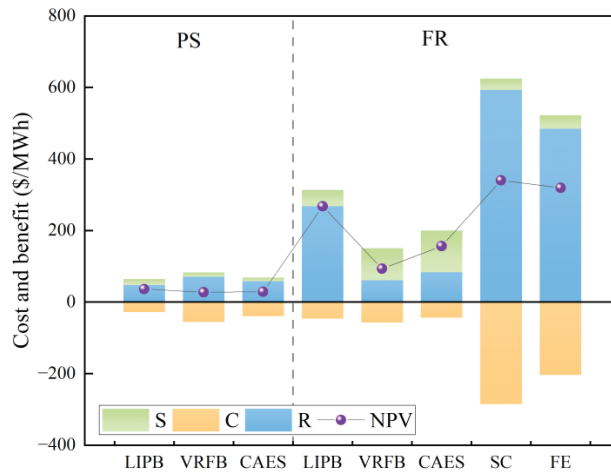


Figure 4: Cost and benefit for ESTs in PS and FR

Moreover, an analysis of the IRR and PP was conducted. IRR' and PP' were examined in scenarios where the carbon mitigation benefit was not considered, as illustrated in Figures 5 and 6. In the PS scenario, the IRR' of LIPB, VRFB, and CAES were 8.94%, 9.15%, and 14.45%, respectively, with corresponding PP' values of 7.7, 12.7, and 15.3 years. After the carbon mitigation benefit being considered, the average increase in IRR' was 4%, accompanied by a 3-year reduction in PP'. In the FR scenario, the IRR' values for LIPB, VRFB, CAES, SC, and FE were 63.1%, 6.1%, 12.3%, 19.8%, and 20.3%, respectively, with corresponding PP' values of 1.7, 17.7, 10.6, 5.5, and 5.6 years. Notably, VRFB exhibited the lowest IRR', while its PP' was the maximum among the considered technologies. When carbon mitigation benefit was considered, the IRR of VRFB and CAES increased by 18.6% and 19.6%, and their PP decreased by 13 and 7 years. However, SC and FE were minimally affected by the carbon mitigation benefit, with IRR increases of 1.37% and 1.81%, and PP decreases of 0.3 and 0.5 years, respectively. LIPB demonstrated the best performance in terms of IRR and PP in both scenarios. The IRR of LIPB in PS was 21.3% and PP was five years, while the IRR in FR was as high as 74%, PP could be realized within two years. With the growth of technology maturity, the cost of LIPB was reduced and the mileage benefit was favorable.

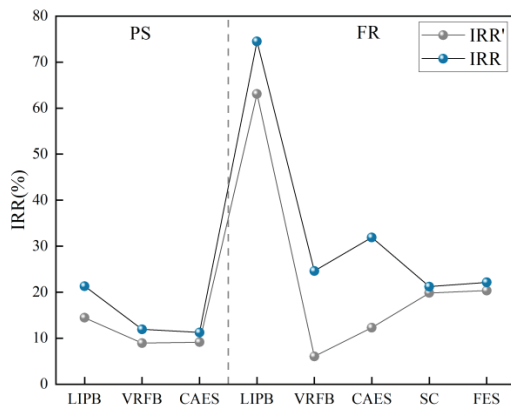


Figure 5: IRR for ESTs in PS and FR

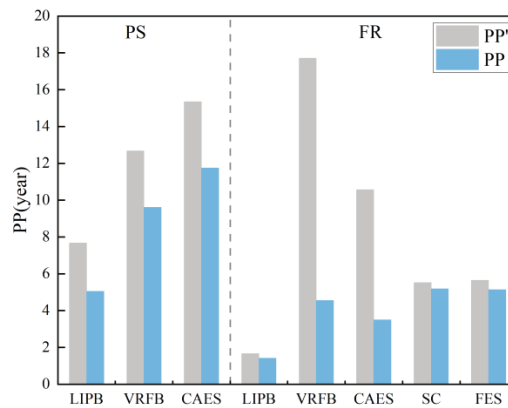


Figure 6: PP for ESTs in PS and FR

3.3 Combination Benefit of Shared Energy Storage

Taking LIPB as an example, the costs and various benefit of independent shared energy storage plants participating in PS and FR auxiliary services were calculated separately as in Figure 7(a, b), and then

the benefit of the energy storage plants was analyzed under different combination patterns, as in Figure 7(c, d). When the LIPB offered PS ancillary service, the cost was 28.1 \$/MWh. Among the five types of benefit, the largest benefit was obtained from PS benefit, followed by capacity leasing, and capacity compensation was negligible with its small size. Among the combination patterns P1, P2, and P3, the highest benefit was obtained from P2 when the EST provided PS service and leasing service. A new proposed combination pattern, P4, generated a net benefit of 84.7 \$/MWh, which was increased by 27.9% compared to existing combination pattern P2. When LIPB provided FR ancillary services, the cost was 46.2 \$/MWh and the maximum benefit was obtained from FR. Among P1, P2, and P3 patterns, the largest benefit was obtained from P2 when the EST provided FR service while participated in the electricity spot market. The benefit was 456.1 \$/MWh in P4, which was 34.3% higher compared to P2. Therefore, if the EST could serve more subjects and participate in more services at the same time, the benefit would be more considerable.

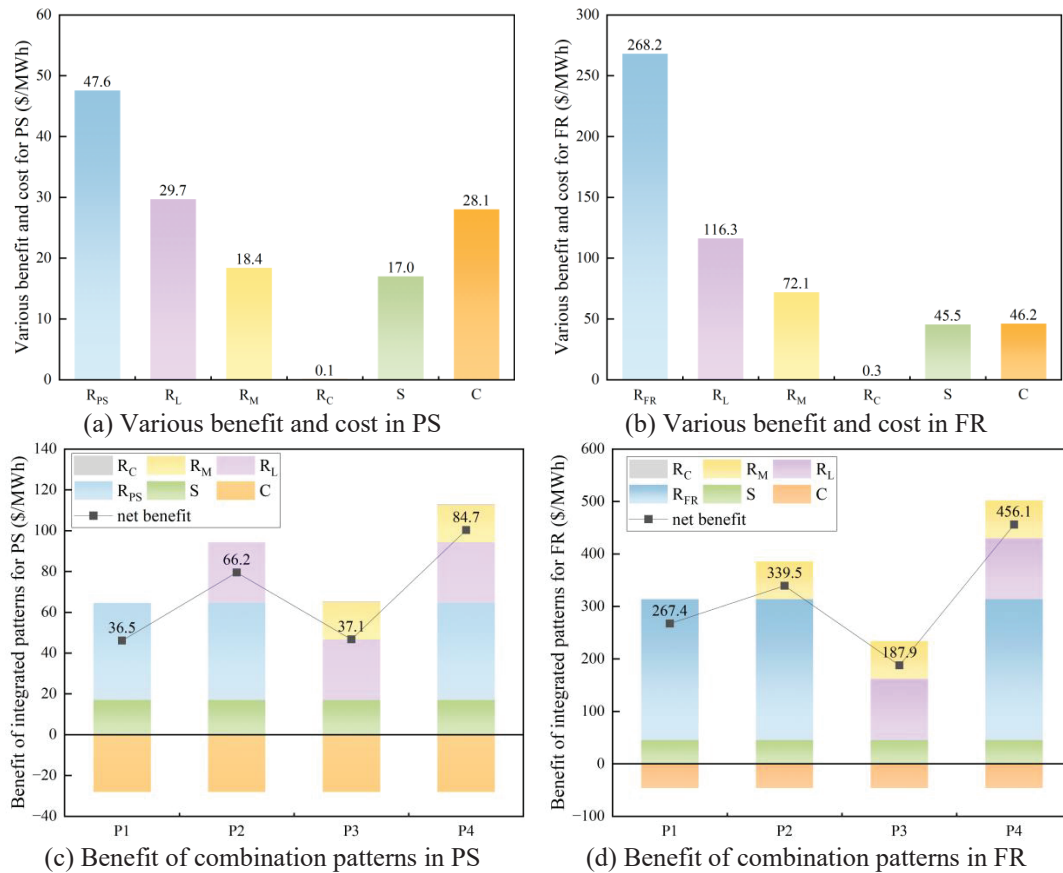


Figure 7: Cost and various benefit of combination patterns

3.4 Parametric Analysis

The influence of critical parameters on NPV and PP were investigated, including energy cost (E_C), carbon tax (T_C), peak-to-valley electricity price gap ($G_{P(t)}$), and comprehensive regulation performance indicator (K). The sensitivity analysis was performed by taking LIPB as an example to change the value of each parameter to analyze the influence on the results.

The influence of E_C on NPV and PP in both scenarios was depicted in Figure 8. For every 100 \$/MWh increased in E_C , the NPV decreased by 12 \$/MWh, and the PP increased by 3.4 years in the PS scenario and 0.5 years in the FR scenario. It indicated that the PP of the PS scenario was greatly affected by E_C . If the energy cost of ESTs decreases it will significantly increase the investibility of energy storage

projects that provide assisted PS. An increase in T_C would result in significant carbon mitigation benefit. the influence of T_C on NPV and PP in both scenarios was presented in Figure 9. For every 50 \$/t increase in T_C , the NPV of the PS and FR scenarios increased by 17 \$/MWh, 45 \$/MWh, and the PP was shortened by 4 years and 0.2 years, respectively. Therefore, T_C has a large impact on the NPV of the FR scenario, but has a large impact on the PP of the PS scenario.

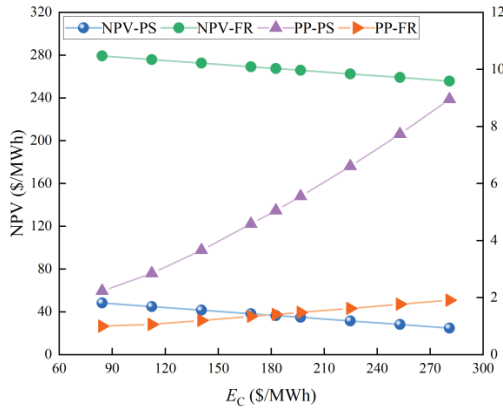


Figure 8: Influence of E_C on NPV and PP

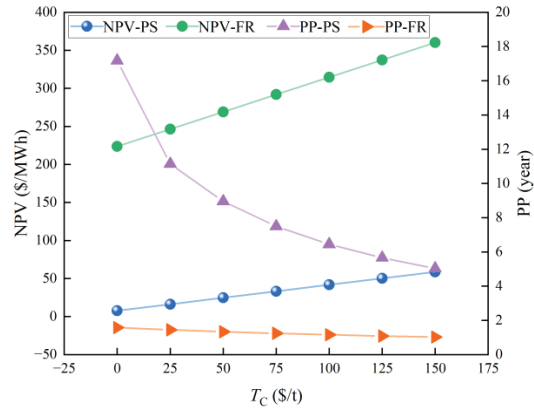


Figure 9: Influence of T_C on NPV and PP

Furthermore, the economic benefit of the PS scenario was mainly affected by the price gap between peak and valley power, and thus $G_{P(t)}$ was analysed as in Figure 10. When $G_{P(t)}$ increased by every 0.1 \$/kWh, the NPV in PS scenario increased by 44.8 \$/MWh and the PP was shortened by 5.3 years. It is evident that the larger the gap in electricity price during peak and valley periods is, the more profit the EST obtains. K was an index that indicated the performance of FR, the larger K was, the better the regulation performance was and the higher the economic efficiency was. The influence of K on the NPV and PP of the FR scenario was depicted in Figure 11. For every increase of K by one, the NPV increased by 134.0 \$/MWh, and PP was shortened by 0.01 year. The results show that K has a large effect on NPV but a minor effect on PP .

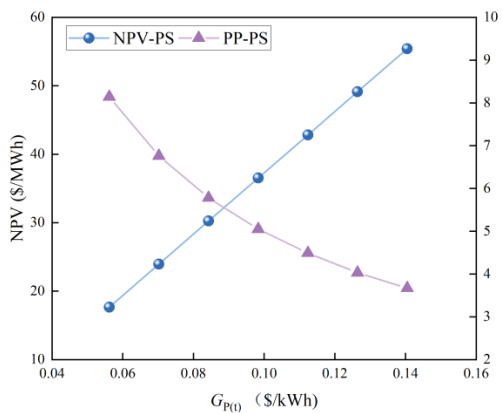


Figure 10: Influence of $G_{P(t)}$ on NPV and PP

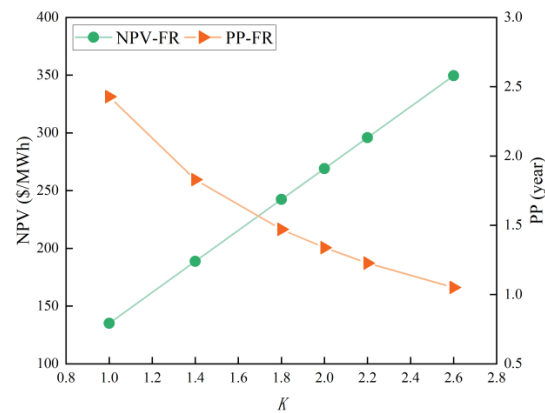


Figure 11: Influence of K on NPV and PP

4 CONCLUSIONS

With the rapid scale-up in popularity of renewable energy sources, the stability of new power systems is under challenge. The integration of ESTs into new power system becomes an effective solution. Therefore, a capacity optimization model for ESTs operating jointly with thermal power plants on the

generation side was developed in the present work. The capacity allocation and benefit of ESTs were analyzed when the benefit was maximized in different scenarios. In addition, a combined benefit model for shared energy storage was proposed and calculated. Finally, parametric analysis was performed. The conclusions were obtained as:

- The EARs in most scenarios were between 2.50%-5.65%, except for the FR scenario where the EARs for VRFB and CAES were less than 1%. The results were informative to the studies of energy storage capacity allocation for assisting thermal power plants in PS and FR. The EARs of VRFB and CAES were miniscule in FR, because their technical characteristics were suitable for long-time energy storage, and they can't be advantageous in FR.
- Co-benefit of FR are more favorable than that of PS. It was obvious that capacity-based ESTs such as CAES and VRFB were more suitable for PS, and power-based ESTs were more suitable for FR. Carbon mitigation benefit accounted for 18-48% of all benefit. It was evident that this was a part that cannot be ignored. The best performer for both IRR and PP in two scenarios was LIPB, which can achieve 1.4 years of recovery in FR.
- For the new proposed combination pattern P4, the shared energy storage offering auxiliary PS and FR obtained benefit of 84.7 \$/MWh and 456.1 \$/MWh, which was 27.9% and 3.3% higher than the highest benefit of the existing combination pattern P2, respectively. The benefit of shared ESTs will be considerable.
- A further sensitivity analysis demonstrated that *PP* in the PS scenario was significantly affected by each factor, and the *NPV* in the FR scenario was more sensitive to T_C than that in the PS scenario, with the change in *NPV* in FR nearly three times as much as that in PS for every 50 \$/t increase in T_C . This implies that greater efforts in raising the carbon tax should be paid.

REFERENCES

- Arbabzadeh, M., Sioshansi, R., Johnson, J.X., et al., 2019, The Role of Energy Storage in Deep Decarbonization of Electricity Production, *Nat. Commun.*, vol. 10: p.3909.
- Baumann, M., Peters, J.F., Weil, M., et al., 2017, CO₂ Footprint and Life-Cycle Costs of Electrochemical Energy Storage for Stationary Grid Applications, *Energy Technol.*, vol. 5, no. 7: p. 1071-1083.
- Bradbury, K., Pratson, L., Patiño-Echeverri, D., 2014, Economic Viability of Energy Storage Systems Based on Price Arbitrage Potential in Real-time U.S. Electricity Markets, *Appl. Energy*, vol. 114: p. 512-519.
- Chowdhury, J.I., Balta-Ozkan, N., Goglio, P., et al., 2020, Techno-environmental Analysis of Battery Storage for Grid Level Energy Services, *Renew. Sust. Energy Rev.*, vol. 131: p.110018.
- Dong, Y., Hauschild, M., Sørup, H., et al., 2019, Evaluating the Monetary Values of Greenhouse Gases Emissions in Life Cycle Impact Assessment, *J. Clean Prod.*, vol. 209: p. 538-549.
- Dreidy, M., Mokhlis, H., Mekhilef, S., 2017, Inertia Response and Frequency Control Techniques for Renewable Energy Sources: A review, *Renew. Sust. Energy Rev.*, vol. 69: p. 144-155.
- Elzein, H., Dandres, T., Levasseur, A., et al., 2019, How Can an Optimized Life Cycle Assessment Method Help Evaluate the Use Phase of Energy Storage Systems? *J. Clean Prod.*, vol. 209: p. 1624-1636.
- Fang, J.C., Xu, Q.S., Xia, Y.X., et al., 2022, Research on Super-capacitor Fast Power Control System, *Energy Rep.*, vol. 8: p. 710-717.
- Han, X.Q., Li, Y.X., Nie, L., et al., 2023, Comparative life cycle greenhouse gas emissions assessment of battery energy storage technologies for grid applications, *J. Clean Prod.*, vol. 392: p. 136251.
- He, G.N., Chen, Q.X., Kang, C.Q., et al., 2016, Optimal Bidding Strategy of Battery Storage in Power Markets Considering Performance-Based Regulation and Battery Cycle Life, *IEEE Trans. Smart Grid*, vol. 7, no.5: p. 2359-2367.
- Hittinger, E., Ciez, R.E., 2020, Modeling Costs and Benefits of Energy Storage Systems, *Annu. Rev. Environ. Resour.*, vol. 45: p. 445-469.
- Jiao, Y., Månsson, D., 2023, Greenhouse Gas Emissions from Hybrid Energy Storage Systems in Future 100% Renewable Power Systems – A Swedish Case Based on Consequential Life Cycle Assessment, *J. Energy Storage*, vol. 57: p. 106167.

- Kong, S.H., Wang, Y.C., Xie, D.W., 2023, Battery Energy Scheduling and Benefit Distribution Models under Shared Energy Storage: A Mini Review, *Front. Energy Res.*, vol. 11: p. 1100214.
- Koohi-Fayegh, S., Rosen, M.A., 2020, A Review of Energy Storage Types, Applications and Recent Developments, *J. Energy Storage*, vol. 27: p. 101047.
- Li, S.J., Xu, Q.S., Huang, J.Y., 2023, Research on the Integrated Application of Battery Energy Storage Systems in Grid Peak and Frequency Regulation, *J. Energy Storage*, vol. 59: p. 106459.
- Lombardi, P., Schwabe, F., 2017, Sharing Economy as a New Business Model for Energy Storage Systems, *Appl. Energy*, vol. 188: p. 485-496.
- Miller, I., Gençer, E., O Sullivan, F., 2018, A General Model for Estimating Emissions from Integrated Power Generation and Energy Storage. Case Study: Integration of Solar Photovoltaic Power and Wind Power with Batteries, *Processes*, vol. 6, no. 12: p. 267.
- Mostafa, M.H., Abdel Aleem, S.H.E., Ali, S.G., et al., 2020, Techno-Economic Assessment of Energy Storage Systems Using Annualized Life Cycle Cost of Storage (LCCOS) and Levelized Cost of Energy (LCOE) Metrics, *J. Energy Storage*, vol. 29: p. 101345.
- Rahman, M.M., Gemechu, E., Oni, A.O., et al., 2021, The Greenhouse Gas Emissions' Footprint and Net Energy Ratio of Utility-scale Electro-Chemical Energy Storage Systems, *Energy Conv. Manag.*, vol. 244: p. 114497.
- Rayit, N.S., Chowdhury, J.I., Balta-Ozkan, N., 2021, Techno-Economic Optimisation of Battery Storage for Grid-Level Energy Services Using Curtailed Energy from Wind, *J. Energy Storage*, vol. 39: p. 102641.
- Ryan, N.A., Lin, Y., Mitchell-Ward, N., et al., 2018, Use-Phase Drives Lithium-Ion Battery Life Cycle Environmental Impacts When Used for Frequency Regulation, *Environ. Sci. Technol.*, vol. 52, no. 17: p. 10163-10174.
- Schram, W.L., AlSkaif, T., Lampropoulos, I., et al., 2020, On the Trade-Off Between Environmental and Economic Objectives in Community Energy Storage Operational Optimization, *IEEE Trans. Sustain. Energy*, vol. 11, no. 4: p. 2653-2661.
- Shi, Y.Y., Xu, B.L., Wang, D., et al., 2018, Using Battery Storage for Peak Shaving and Frequency Regulation: Joint Optimization for Superlinear Gains, *IEEE Trans. Power Syst.*, vol. 33, no.3: p. 2882-2894.
- Stroe, D., Swierczynski, M., Stroe, A., et al., 2016, Degradation Behavior of Lithium-Ion Batteries Based on Lifetime Models and Field Measured Frequency Regulation Mission Profile, *IEEE Trans. Ind. Appl.*, vol. 52, no. 6: p. 5009-5018.
- Sufyan, M., Rahim, N.A., Aman, M.M., et al., 2019, Sizing and Applications of Battery Energy Storage Technologies in Smart Grid System: A Review, *J. Renew. Sustain. Energy*, vol. 11, no.1: p. 014105.
- Tian, S., He, H.Y., Kendall, A., et al., 2021, Environmental Benefit-Detriment Thresholds for Flow Battery Energy Storage Systems: A Case Study in California, *Appl. Energy*, vol. 300: p. 117345.
- Wang, W., Yuan, B.Q., Sun, Q., et al., 2022, Application of Energy Storage in Integrated Energy Systems — A Solution to Fluctuation and Uncertainty of Renewable Energy, *J. Energy Storage*, vol. 52: p. 104812.
- Zakeri, B., Syri, S., 2015, Electrical Energy Storage Systems: A Comparative Life Cycle Cost Analysis, *Renew. Sust. Energy Rev.*, vol. 42: p. 569-596.
- Zhang, Y.X., Xu, Y., Yang, H.M., et al., 2020, Optimal Whole-Life-Cycle Planning of Battery Energy Storage for Multi-Functional Services in Power Systems, *IEEE Trans. Sustain. Energy*, vol. 11, no. 4: p. 2077-2086.

ACKNOWLEDGEMENT

This work was supported by the National Key R&D Program (2022YFB4202403) and the Natural Science Basic Research Plan in Shaanxi Province of China (No. 2023-JC-YB-444).